

# DN-ResNet: Efficient Deep Residual Network for Image Denoising

Haoyu Ren, Mostafa El-khamy, Jungwon Lee

SOC R&D, Samsung Semiconductor Inc.  
4921 Directors Pl, San Diego, CA 92121, USA  
{haoyu.ren,mostafa.e,jungwon2.lee}@samsung.com

**Abstract.** A deep learning approach to blind denoising of images without complete knowledge of the noise statistics is considered. We propose DN-ResNet, which is a deep convolutional neural network (CNN) consisting of several residual blocks (ResBlocks). With cascade training, DN-ResNet is more accurate and more computationally efficient than the state of art denoising networks. An edge-aware loss function is further utilized in training DN-ResNet, so that the denoising results have better perceptive quality compared to conventional loss function. Next, we introduce the depthwise separable DN-ResNet (DS-DN-ResNet) utilizing the proposed Depthwise Seperable ResBlock (DS-ResBlock) instead of standard ResBlock, which has much less computational cost. DS-DN-ResNet is incrementally evolved by replacing the ResBlocks in DN-ResNet by DS-ResBlocks stage by stage. As a result, high accuracy and good computational efficiency are achieved concurrently. Whereas previous state of art deep learning methods focused on denoising either Gaussian or Poisson corrupted images, we consider denoising images having the more practical Poisson with additive Gaussian noise as well. The results show that DN-ResNets are more efficient, robust, and perform better denoising than current state of art deep learning methods, as well as the popular variants of the BM3D algorithm, in cases of blind and non-blind denoising of images corrupted with Poisson, Gaussian or Poisson-Gaussian noise. Our network also works well for other image enhancement task such as compressed image restoration.

**Keywords:** Denoising, Depth-aware, Cascade involving, ResNet, CNN

## 1 Introduction

Denoising is an active topic in image processing since it is a key step in many practical applications, such as image and video capturing. It aims to generate a clean image  $X$  from a given noisy image  $Y$  which follows an image degradation model  $Y = D(X)$ . For the widely used additive Gaussian noise (AWGN) model, the  $i$ th observed pixel is

$$y_i = D(x_i) = x_i + n_i \quad (1)$$

where  $n_i \sim \mathcal{N}(0, \sigma^2)$  is i.i.d Gaussian noise with zero mean and variance  $\sigma^2$ . AWGN has been used to model the signal-independent thermal noise and other system imperfections. Degradation due to low light shot noise is signal dependent and has often been modeled using Poisson noise

$$y_i = D(x_i) = p_i, \quad p_i \sim \mathcal{P}(x_i) \quad (2)$$

where  $\mathcal{P}(x_i)$  is a Poisson random variable with mean  $x_i$ . However, this noise approaches a Gaussian distribution for average light conditions as  $\mathcal{P}(\lambda) \approx \mathcal{N}(\lambda, \lambda)$ , for large enough  $\lambda$ . Hence, the noise due to capturing by an imaging device is better modeled as a Poisson noise with AWGN, referred to as Poisson-Gaussian noise, such that

$$y_i = D(x_i) = \alpha p_i + n_i, \quad \alpha > 0 \quad (3)$$

which has been verified by experimental results [7].

Recently, the state of art denoising accuracy is achieved by deep neural networks [26][22], which construct a mapping between the noisy image and clean image. Unfortunately, most of existing denoising networks cannot be executed in real-time due to their large network size. In addition, it is relatively difficult to set the hyperparameters when learning a very deep network, such as the weight initialization, the learning rate, and the weight decay rate. With inappropriate parameters, the training might fall into local minimum or not converge at all.

In this paper, we propose a Denoising Residual Network (DN-ResNet) which is more efficient and accurate than prior art. DN-ResNet consists of residual blocks (ResBlock) which are gradually inserted into the network stage by stage during the training. This training strategy not only allows the resulting DN-ResNet to converge faster, but also allows it to be more computationally efficient than prior art denoising networks. Even better perceptive quality have been observed by using the proposed edge-aware loss function instead of the conventional mean square error (MSE). In addition, we introduce the depthwise separable ResBlock (DS-ResBlock) into DN-ResNet to construct the depthwise separable ResNet (DS-DN-ResNet). DS-DN-ResNet is generated by the proposed incremental evolution from DN-ResNet, where the ResBlocks in DN-ResNet are replaced by DS-ResBlocks stage by stage. As a result, we may obtain a 2.5 times complexity reduction for DN-ResNet, with less than 0.1 dB PSNR loss. To our knowledge, DN-ResNet is the first unified deep CNN trained for the problem of blind denoising of images corrupted by multiple type of noises. By cascading only 5 ResBlocks, DN-ResNet and DS-DN-ResNet achieve the state of art performance on all three denoising problems, Gaussian, Poisson, and Poisson-Gaussian, for both cases of non-blind denoising (known noise level for noisy input) and blind denoising (unknown noise level for noisy input). The speed is also much faster than prior art denoising networks. Moreover, we show that DN-ResNet works well for compressed image restoration. This implies that DN-ResNet can be generalized to other applications.

As summary, our contributions are three folds:

1. We show that ResNet is effective for image denoising, and using edge-aware loss function significantly improves the perceptive quality. The resulting DN-ResNet achieves the state of art accuracy, and is 4 times less complicate than existing networks;
2. We introduce the depthwise separable ResBlock (DS-ResBlock) to construct DS-DN-ResNet. The incrementally evolved DS-DN-ResNet is 2.5 times faster than DN-ResNet, without significant accuracy loss;
3. We show that the proposed DN-ResNet works well for all types of noises, even without knowing the noise level. It can be generalized to other image enhancement task such as compressed image restoration;

## 2 Related work

### 2.1 Image denoising

During the past years, numerous approaches have been exploited for modeling image priors for denoising, such as nonlocal self-similarity (NSS) [8] and sparse coding [5]. The block matching with 3D collaborative filtering (BM3D) [4] and its variants such as iterative BM3D with variance stabilizing transforms (I+VST+BM3D) [1] and generalized Anscombe variance stabilizing transform with BM3D (GAT-BM3D) [13] are widely used. These methods generally involve a complex optimization problem in the testing stage, which makes the denoising process time-consuming. To improve the efficiency, learning-based methods are proposed to get rid of the iterative optimization procedure, such as the trainable nonlinear reaction diffusion (TNRD) [3], and Gaussian conditional random field [20] for non-blind image deblurring. Unfortunately, the accuracy of these methods is still limited due to the use of specific image prior. It is also difficult to set the handcrafted parameters during the stage-wise learning.

Recently, deep neural networks have been deployed for image denoising due to their significant improvement of the accuracy [2]. Zhang et al. [26] constructed a 20-layer feed-forward denoising convolutional neural networks with residual learning for Gaussian denoising. Remez et al. trained 20-layer CNNs for each object category respectively and showed good performance for either Gaussian denoising [15] or Poisson denoising [16]. Zhang et al. [27] proposed FFDNet adopting orthogonal regularization to enhance the generalization ability of Gaussian denoising. Tai et al. designed MemNet [22], where the feature map concatenations and skip connections are utilized to construct a network for image super resolution, Gaussian denoising, and JPEG deblocking.  $1 \times 1$  convolutions are adopted to integrate the long-term memorization, which shows significant accuracy improvements. Most of the existing networks are designed for single type of noise only. Due to the high computational cost, they can not be executed in real-time. In contrast, our DN-ResNet is far more efficient. The same network architecture can be utilized for Gaussian, Poisson, and Poisson-Gaussian noise, as well as other image enhancement tasks.

## 2.2 Deep learning based compressed image restoration

Compressed image restoration aims to reduce the artifacts of decoded compressed images, so that the images can be stored or transmitted at low bit rates. Most of existing work design an end-to-end network including both the encoding (compression) and decoding procedure. Toderici et al. [24] presented a set of full-resolution lossy image compression methods using recurrent neural network based encoder and decoder with entropy coding. Theis et al. [23] constructed the compression network by deep autoencoders with a sub-pixel structure. In these work, although a low bit rate can be achieved, both of the encoding and decoding procedure are replaced by deep neural networks. As a result, it is difficult to integrate them into real system, where efficient image compression algorithms such as JPEG are implemented. In this paper, we consider the compressed image restoration as a ‘denoising’ problem, where the noise comes from image compression algorithms. DN-ResNet is trained to refine the quality of decoded compressed image. Since our network can be considered as a post-processing step, it can be applied to any existing image compression algorithms.

## 3 Denoising Residual Network

### 3.1 DN-ResNet

We aim to train a deep convolution neural network for image denoising. The network takes a noisy image  $Y$  as input and predicts a clean image  $X$  as its output. Given a training set  $\{X_i, Y_i\}, i = 1, \dots, N$  with  $N$  samples, our goal is to learn a model  $S$  that predicts the clean image  $\hat{X}_i = S(Y_i)$ .

ResNet [9] has demonstrated considerable performance in computer vision applications such as image classification. The basic element of our proposed denoising residual network (DN-ResNet) is a simplified ResBlock, as shown in Fig. 1(b). Different from the standard ResBlock in Fig. 1(a), we remove the batch normalization layers and the ReLU layer after the addition, because removing these layers will not harm the performance of feature-map based ResNet [12].

We construct our DN-ResNet by concatenating the ResBlocks in Fig. 1(b). We observed that as the network goes deeper, the training and the hyperparameter tuning become more difficult. To solve this problem, we follow the cascade training [18], which separates the whole training into stages and proceeds one by one. The training of DN-ResNet starts from a simple 3-layer CNN model. The first layer consists of  $64 \ 9 \times 9$  filters. The second layer consist of  $32 \ 5 \times 5$  filters. There is only one  $5 \times 5$  filter in the last layer. All convolutions have stride one, and all the weights are randomly initialized from a Gaussian distribution with  $\sigma = 0.001$ . After the 3-layer CNN is trained, we start cascading the ResBlocks stage by stage, as shown in Fig. 2. When the training of current stage is finished, e.g., the training loss of current stage is 3% lower than previous stage, the training will proceed to next stage, and the network is cascaded to a deeper network. In each stage, one new ResBlock is inserted. So the training starts from 3 layers, and proceeds to 5 layers, 7 layers, etc.. Each convolutional layer in the

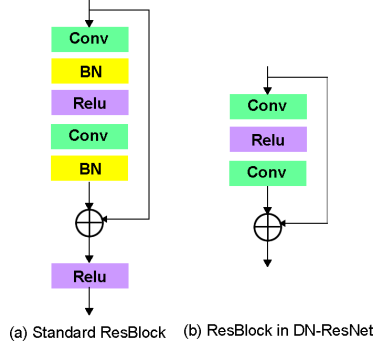


**Fig. 1.** ResBlocks in DN-ResNet. (a) Standard ResBlock (b) ResBlock in DN-ResNet.

ResBlock consists of  $32\ 3 \times 3$  filters. It ensures a smaller network when going deeper. The new layers are inserted just before the last  $5 \times 5$  layer. The weights of pre-existing layers are inherited from the previous stage, and the weights of the new ResBlocks are randomly initialized (Gaussian with  $\sigma = 0.001$ ). Hence, only a few weights of DN-ResNet are randomly initialized at each stage, so the convergence will be relatively easy. We find that using a fixed learning rate 0.0001 for all layers without any decay is feasible.

Since new convolutional layers will reduce the size of the feature map, we zero pad 2 pixels in each new  $3 \times 3$  layer. As a result, all the stages in cascade training have the same size as the output, so that the training samples could be shared. When cascading 5 ResBlocks, the resulting DN-ResNet will have  $5 \times 2 + 3 = 13$  convolutional layers. Our experiments show that such DN-ResNet-13 has already achieved the state of art accuracy on all type of noises.

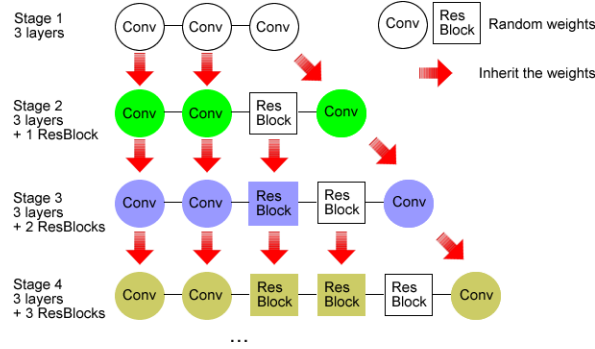


**Fig. 2.** Cascade training of DN-ResNet. Circle denotes standard convolutional layer, rectangle denotes ResBlock.

### 3.2 Depthwise separable DN-ResNet

In this section, we propose depthwise separable DN-ResNet (DS-DN-ResNet) to further reduce the network size of DN-ResNet, as well as the computational cost. In the classification network MobileNet [10][19], the standard convolutional layer is factorized into a depthwise convolution and a  $1 \times 1$  pointwise convolution, which achieves significant efficiency gain. As shown in Fig. 3, the standard convolution with  $M$  input channels and  $N$   $K \times K$  filters is replaced by a depthwise convolution layer with  $M$   $K \times K$  filters, and a pointwise convolution layer with  $N$   $1 \times 1$  convolutional filters and  $M$  input channels. Assume the input feature map size is  $W \times H$ , the number of the multiplications are reduced from  $M \times K \times K \times N \times W \times H$  to  $M \times K \times K \times W \times H + M \times N \times W \times H$ .

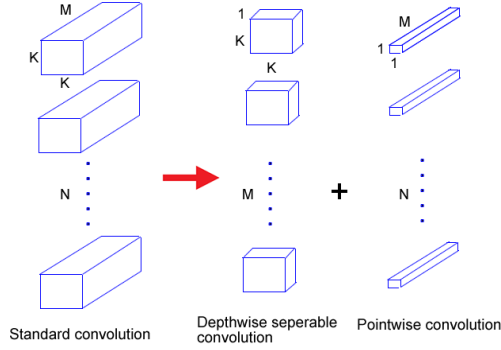


**Fig. 3.** Depthwise separable convolution. The standard convolution (left) is replaced by depthwise convolution (middle) and pointwise convolution (right).

Inspired by this idea, we propose the depthwise separable ResBlock (DS-ResBlock), as shown in Fig. 4. In DS-ResBlock, the standard convolutional layers in ResBlock are replaced by depthwise separable convolutional layers and pointwise convolutional layers. Relu activation is added for all the convolutional layers in DS-ResBlock. Assume the size of input feature map is  $640 \times 480$ , the number of the multiplications in the ResBlock in Fig. 4(a) is  $640 \times 480 \times 3 \times 3 \times 32 \times 32 \times 2 = 5.6 \times 10^9$ . In the corresponding DS-ResBlock in Fig. 4(b), the number of multiplications is  $640 \times 480 \times 3 \times 3 \times 32 + 640 \times 480 \times 32 \times 32 = 9 \times 10^8$ . The computational cost is reduced 6 times.

To train DS-DN-ResNet, one intuitive way is to apply cascade training from scratch. Since we have already trained the DN-ResNet, we describe another way to obtain DS-DN-ResNet to save training time, which is called ‘incremental evolution’. To obtain a DS-DN-ResNet from existing DN-ResNet, a feasible way is to replace all ResBlocks by DS-ResBlocks, and fine-tune the whole network. If this procedure is done in a one-shot way, the fine-tuning will not converge well (see Table 3 for details). In the incremental evolution, the ResBlocks are replaced stage by stage. In each stage, only one-ResBlock is replaced by DS-ResBlock,

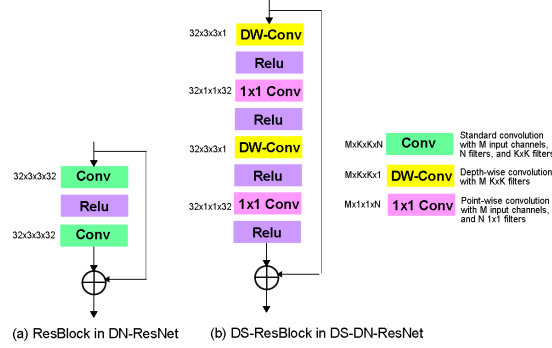


**Fig. 4.** Comparison between the ResBlock in DN-ResNet and the DS-ResBlock in DS-DN-ResNet.

and followed by a fine-tuning, as shown in Fig. 5. Similar to cascade training, the weights in the new DS-ResBlock are randomly initialized, and the weights in all other layers are inherited. The replacement starts from the tail side to ensure a smaller influence to the whole network. In the implementation, we first train 13-layer DN-ResNet, and then evolve it to DS-DN-ResNet. The learning rate is the same as cascade training. The fine-tuning will last 10 epochs for each evolution stage.

After incremental evolution, there are still three standard convolutional layers (1st, 2nd, and the last one) in DS-DN-ResNet. The overall complexity of DS-DN-ResNet is about 2.5 times less compared to DN-ResNet, without significant accuracy loss ( $< 0.1$  dB PSNR, see Table 3 for details). We do not replace the 1st and 2nd standard convolutional layers by depthwise version because it will decrease the accuracy a lot ( $> 0.3$  dB PSNR).

### 3.3 Edge-aware loss function

Most of existing denoising networks aim to minimize the Mean Square Error (MSE)  $\frac{1}{N} \sum_{i=1}^N \|X_i - \hat{X}_i\|^2$  over the training set. In this paper, we propose an edge-aware loss function, where the pixels in the edges are granted higher weights compared to non-edge pixels

$$loss = \frac{1}{N} \sum_{i=1}^N \|X_i - \hat{X}_i\|^2 + w \times \frac{1}{N} \sum_{i=1}^N \|X_i M_i - \hat{X}_i M_i\|^2. \quad (4)$$

In Eq. (4),  $X_i$  is the ground truth of  $i$ th clean image,  $\hat{X}_i$  is the  $i$ th denoised image,  $M$  is an edge map,  $N$  is the number of images, and  $w$  is a constant to control the trade-off between edge and non-edge pixels.

There are two advantages of applying such edge-aware loss function. Firstly, one of the major challenge in image denoising is that the edges are difficult to be retrieved from a noisy image, especially when the noise level is high. Adding

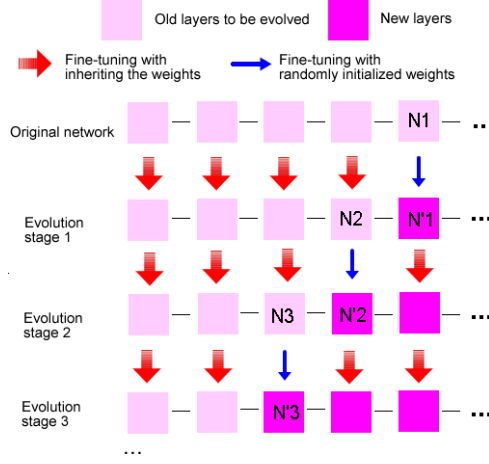


**Fig. 5.** Incremental evolution from DN-ResNet to DS-DN-ResNet.

a corresponding constraint in the loss function is reasonable. Secondly, the high-frequency information such as edge is very sensitive in human vision. Increasing the denoising accuracy of edge pixels will contribute to the perceptive quality.

We try two ways to construct  $M$ , including (a) gradient magnitude from Sobel filter, and (b) binary edge mask by thresholding (a). In the experiments, we show that using such edge-aware loss function can grant us better perceptive quality. The SSIM (structural similarity measure) is significantly improved.

**Table 1.** PSNR (dB) evaluation of DN-ResNets with different layers for different denoising problems on PASCAL VOC 2010 dataset. Noise level is known. Bold fold indicates the best. Conventional MSE loss function is utilized for all models.

DN-ResNet	sigma/peak	3-layer	5-layer	7-layer	9-layer	11-layer	13-layer	13-layer-os
Parameters	-	57,184	75,616	94,048	112,480	130,912	149,344	149,344
Gaussian	10	34.43	34.56	34.71	34.80	34.93	<b>34.99</b>	34.70
	25	29.86	30.03	30.10	30.30	30.44	<b>30.52</b>	30.27
	50	26.86	27.05	27.22	27.29	27.38	<b>27.50</b>	27.14
	75	25.24	25.43	25.55	25.63	25.81	<b>25.89</b>	25.61
Poisson	1	22.51	22.66	22.74	22.88	22.95	<b>23.06</b>	22.80
	2	23.66	23.74	23.92	24.05	24.14	<b>24.23</b>	23.96
	4	24.67	24.80	24.91	25.14	25.27	<b>25.39</b>	25.01
	8	26.01	26.24	26.35	26.55	26.64	<b>26.77</b>	26.49
Poisson-Gaussian	0.1/1	22.11	22.27	22.36	22.50	22.65	<b>22.73</b>	22.30
	0.2/2	22.99	23.14	23.22	23.40	23.59	<b>23.75</b>	23.44
	0.5/5	24.54	24.61	24.77	24.90	25.00	<b>25.10</b>	24.78
	1/10	25.61	25.69	25.77	25.91	25.99	<b>26.14</b>	25.67
	2/20	26.59	26.71	26.89	26.99	27.14	<b>27.29</b>	26.88
	3/30	27.10	27.22	27.37	27.50	27.61	<b>27.77</b>	27.41
	6/60	27.87	27.98	28.16	28.32	28.48	<b>28.59</b>	28.11
	12/120	28.19	28.30	28.44	28.58	28.72	<b>28.88</b>	28.50



**Table 2.** PSNR (dB)/SSIM evaluation of 13-layer DN-ResNets with different loss functions and blind/non-blind denoising. Bold fold indicates the best SSIM. ‘edge’ means the network is trained by edge-aware loss function. In ‘edge-a’, the edge map in the edge-aware loss function is the gradient magnitude from Sobel filter. In ‘edge-b’, the edge map is a binary mask by thresholding the Sobel map with 150. We have tried different thresholds to obtain the binary edge mask and find that 150 is the best one.

DN-ResNet	sigma/peak	non-blind	blind	blind+‘edge-a’	blind+‘edge-b’
Parameters	-	149,344	149,344	149,344	149,344
Gaussian	10	34.99/0.9224	34.88/0.9217	34.88/ <b>0.9271</b>	34.85/0.9266
	25	30.52/0.8383	30.47/0.8369	30.45/ <b>0.8441</b>	30.44/0.8433
	50	27.50/0.7464	27.44/0.7458	27.41/0.7499	27.42/ <b>0.7502</b>
	75	25.89/0.6881	25.80/0.6880	25.80/0.6947	25.77/ <b>0.6950</b>
Poisson	1	23.06/0.5958	22.99/0.5949	23.00/ <b>0.6050</b>	22.95/0.6038
	2	24.23/0.6403	24.17/0.6377	24.15/ <b>0.6501</b>	24.15/0.6488
	4	25.39/0.6858	25.33/0.6829	25.30/ <b>0.6911</b>	25.31/0.6899
	8	26.77/0.7332	26.72/0.7329	26.71/ <b>0.7388</b>	26.71/0.7371
Poisson-Gaussian	0.1/1	22.73/0.5938	22.65/0.5936	22.64/ <b>0.6044</b>	22.60/0.6019
	0.2/2	23.75/0.6345	23.69/0.6337	23.68/ <b>0.6402</b>	23.66/0.6400
	0.5/5	25.10/0.6878	24.98/0.6860	24.95/ <b>0.6955</b>	24.91/0.6933
	1/10	26.14/0.7263	26.07/0.7255	26.05/ <b>0.7334</b>	26.05/0.7330
	2/20	27.29/0.7613	27.18/0.7600	27.15/ <b>0.7677</b>	27.15/0.7659
	3/30	27.77/0.7785	27.64/0.7770	27.59/ <b>0.7844</b>	27.61/0.7840
	6/60	28.59/0.8010	28.51/0.8001	28.50/0.8068	28.50/ <b>0.8077</b>
	12/120	28.88/0.8147	28.80/0.8122	28.77/ <b>0.8180</b>	28.78/0.8166

## 4 Experiments

### 4.1 Experiment setting

For image denoising, we use the PASCAL VOC 2010 dataset [6]. We follow the same training and testing split as [15], 1,000 testing images are used to evaluate the performance of the proposed DN-ResNet, while the remaining images are used for training. Random Gaussian/Poisson/Poisson-Gaussian noisy images are generated with different noise levels. We consider AWGN with different noise variances  $\sigma^2$ , where  $\sigma \in \{10, 25, 50, 75\}$ . We follow the same way as [1][16], before corrupting with Poisson noise, the input image pixel values are scaled to have a max peak value from the set  $peak \in \{1, 2, 4, 8\}$ . For the Poisson-Gaussian noise, we follow the same setting as [13], where  $\sigma \in \{0.1, 0.2, 0.5, 1, 2, 3, 6, 12\}$ ,  $peak = 10 \times \sigma$ .  $33 \times 33$  noisy patches and the corresponding  $17 \times 17$  clean patches are cropped for training. For more comparison to other existing methods, we also use the Set14 [25], and BSD [14] datasets in the testing.

For compressed image restoration, we utilize the dataset provided by the challenge on learned image compression (CLIC) [11]. The commonly-used image compression algorithms, JPEG, JPEG 2000, and BPG (Better Portable Graphics) are utilized to obtain the decoded images.  $33 \times 33$  decoded patches and the corresponding  $17 \times 17$  clean patches are further extracted for training.

Our networks are trained on y/cb/cr channels<sup>1</sup>. For non-blind denoising, multiple networks are trained for each noise level respectively. In contrast, only

<sup>1</sup> In the quantitative evaluation, we show the PSNR/SSIM of the networks trained on y-channel only for fair comparison to existing work.

one DN-ResNet is trained for blind denoising by mixing all training samples corrupted by Gaussian/Poisson/Poisson-Gaussian noises. Peak-Signal-to-Noise-Ratio (PSNR) and SSIM are utilized as evaluation protocol.

**Table 3.** PSNR (dB)/SSIM evaluation of 13-layer DN-ResNets with different Res-Blocks for blind denoising. ‘DN’ is DN-ResNet, ‘DS-DN’ is DS-DN-ResNet constructed by incremental evolution from DN-ResNet. ‘DS-DN-os’ is the DS-DN-ResNet constructed by one-shot fine-tuning from DN-ResNet. ‘edge-a’ denotes that the network is trained by edge-aware loss function. MACs are calculated for  $640 \times 480$  input.

DN-ResNet	sigma/peak	DN	DS-DN	DS-DN-os	DN+‘edge-a’	DS-DN+‘edge-a’
Parameters	-	149,344	63,728	63,728	149,344	63,728
MACs (Billion)	-	45.9	19.6	19.6	45.9	19.6
Gaussian	10	34.88/0.9217	34.79/0.9206	34.41/0.9088	34.88/0.9271	34.79/0.9259
	25	30.47/0.8369	30.36/0.8355	30.00/0.8240	30.45/0.8441	30.36/0.8433
	50	27.44/0.7458	27.34/0.7439	26.99/0.7298	27.41/0.7499	27.32/0.7484
	75	25.80/0.6880	25.74/0.6878	25.32/0.6759	25.80/0.6947	25.72/0.6939
Poisson	1	22.99/0.5949	22.89/0.5933	22.59/0.5870	23.00/0.6050	22.89/0.6040
	2	24.17/0.6377	24.11/0.6364	23.77/0.6302	24.15/0.6501	24.09/0.6499
	4	25.33/0.6829	25.26/0.6811	24.88/0.6733	25.30/0.6911	25.24/0.6899
	8	26.72/0.7329	26.62/0.7314	26.30/0.7265	26.71/0.7388	26.60/0.7377
Poisson-Gaussian	0.1/1	22.65/0.5936	22.57/0.5919	22.17/0.5830	22.64/0.6044	22.56/0.6038
	0.2/2	23.69/0.6337	23.58/0.6322	23.20/0.6269	23.68/0.6402	23.54/0.6389
	0.5/5	24.98/0.6860	24.93/0.6843	24.65/0.6788	24.95/0.6955	24.93/0.6941
	1/10	26.07/0.7255	25.99/0.7239	25.66/0.7188	26.05/0.7334	26.00/0.7330
	2/20	27.18/0.7600	27.12/0.7596	26.80/0.7524	27.15/0.7677	27.11/0.7666
	3/30	27.64/0.7770	27.57/0.7755	27.24/0.7700	27.59/0.7844	27.53/0.7839
	6/60	28.51/0.8001	28.46/0.7991	28.16/0.7929	28.50/0.8068	28.45/0.8061
	12/120	28.80/0.8122	28.74/0.8108	28.44/0.8059	28.77/0.8180	28.68/0.8177

## 4.2 Experiments on image denoising

We first test the DN-ResNets up to 13 layers on non-blind Gaussian, Poisson, and Poisson-Gaussian denoising. These DN-ResNets are trained by cascading the ResBlocks in Fig. 1(b). The conventional MSE loss is utilized for all networks. In Table 1, we find that for all the above three denoising problems, the PSNR consistently increases along with using more layers. Although the deepest network we show is 13-layer DN-ResNet, the accuracy could still be further improved by cascading more layers. This is consistent with ‘the deeper, the better’. We also compare the cascade training versus one-shot training (‘13-layer-os’ in Table 1), where an end-to-end 13-layer DN-ResNet is trained from unsupervised weight initialization. We observe that such one-shot training results in 0.3 dB PSNR degradation compared to cascade training. This result makes sense because cascade training can be considered as a ‘partial-supervised weight initialization’, its convergence will be easier compared to one-shot training based on unsupervised weight initialization.

Next, we test the DN-ResNets trained by edge-aware loss function described in Section 3.3, as well as utilizing DN-ResNet for blind denoising. In Table 2, we observe that utilizing DN-ResNet for blind denoising will not decrease the accuracy much compared to non-blind denoising. This trade-off is valuable since

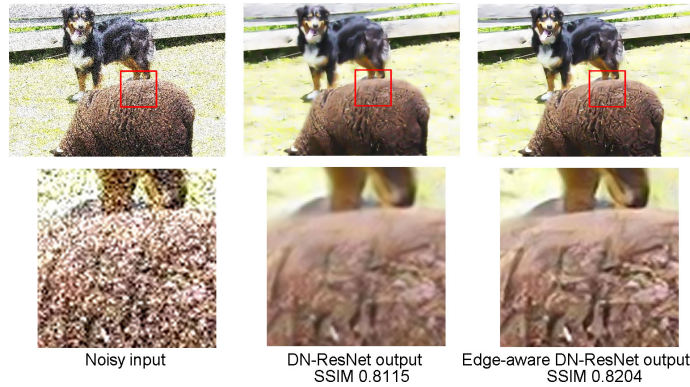


**Fig. 6.** Example outputs of different Poisson-Gaussian blind denoising networks. Left: noisy input. Mid: DN-ResNet output. Right: edge-aware DN-ResNet output.

blind denoising does not require a time-consuming noise level estimation. In addition, we show that utilizing edge-aware loss function (blind+‘edge-a’/‘edge-b’) improves the SSIM 0.005-0.01, without degrading the PSNR much. Since the conventional MSE has the same equation as PSNR, the slightly degradation in PSNR of the edge-aware DN-ResNet is reasonable. Using the edge map generated by Sobel gradient magnitude (blind+‘edge-a’,  $w = 0.025$  in Eq. (5)) is better than binary edge mask (blind+‘edge-b’,  $w = 4$ ). The perceptive quality is clearly improved as well, as illustrated in Fig. 6. It can be seen that the output from edge-aware DN-ResNet has sharper edge and higher SSIM compared to the output from ordinary DN-ResNet. This shows the effectiveness of emphasizing edge pixels during the training.

Moreover, we evaluate the DN-ResNets constructed by different ResBlocks for the blind denoising problem. In Table 3, We observe that the DS-DN-ResNet (DS-DN) decreases less than 0.1 dB PSNR and less than 0.002 SSIM compared to DN-ResNet, but the computational cost (MACs, number of multiplications and accumulations) and the network size are significantly reduced. We also notice that if the DS-DN-ResNet is constructed by one-shot fine-tuning DN-ResNet (DS-DN-os), both the PSNR and SSIM will decrease a lot. This indicates that the proposed incrementally evolved DS-DN-ResNet is able to improve the efficiency of DN-ResNet. Using the DS-ResBlock together with the edge-aware loss function, we can achieve considerable accuracy, good perceptive quality, and less computational cost at the same time.

### 4.3 Comparison to the state of art denoising algorithms

In Table 4, we compare the proposed DN-ResNet to the state of art denoising algorithms in PASCAL VOC dataset. For fair comparison, we retrain other networks using the same VOC dataset. We observe that DN-ResNet-13 blind denoising network clearly outperforms other blind and non-blind Gaussian denois-

**Table 4.** PSNR (dB)/SSIM comparison to the state of art Gaussian/Poisson/Poisson-Gaussian denoising algorithms on PASCAL VOC 2010 dataset.

Gaussian sigma	blind	10	25	50	75
BM3D [4]	No	34.26/0.9197	29.62/0.8294	26.61/0.7404	25.12/0.6852
DN-CNN-3 [26]	Yes	-	29.87/0.8350	26.85/0.7439	-
DN-CNN-S [26]	No	34.79/0.9216	30.23/0.8379	27.29/0.7444	25.58/0.6888
DenoiseNet [15]	No	34.87/0.9219	30.36/0.8388	27.32/0.7447	25.74/0.6899
DN-ResNet-13+‘edge-a’	Yes	<b>34.88/0.9271</b>	<b>30.45/0.8441</b>	<b>27.41/0.7499</b>	<b>25.80/0.6947</b>
DS-DN-ResNet-13+‘edge-a’	Yes	34.79/0.9259	30.36/0.8433	27.32/0.7484	25.72/0.6939
Poisson peak	blind	1	2	4	8
IVST+BM3D [1]	No	22.71/0.5920	23.70/0.6418	24.78/0.6815	26.08/0.7297
DenoiseNet [16]	No	22.87/0.5989	24.09/0.6452	25.26/0.6857	26.70/0.7329
DN-ResNet-13+‘edge-a’	Yes	<b>23.00/0.6050</b>	<b>24.15/0.6501</b>	<b>25.30/0.6911</b>	<b>26.71/0.7388</b>
DS-DN-ResNet-13+‘edge-a’	Yes	22.89/0.6040	24.09/0.6499	25.24/0.6899	26.60/0.7377
Poisson-Gaussian sigma/peak	blind	0.1/1	0.2/2	0.5/5	1/10
GAT+BM3D [13]	No	21.28/0.5451	22.56/0.5795	24.13/0.6478	25.38/0.7008
DN-ResNet-13+‘edge-a’	Yes	<b>22.64/0.6044</b>	<b>23.68/0.6402</b>	<b>24.95/0.6905</b>	<b>26.05/0.7334</b>
DS-DN-ResNet-13+‘edge-a’	Yes	22.56/0.6038	23.54/0.6389	24.93/0.6941	26.00/0.7330
Poisson-Gaussian sigma/peak	blind	2/20	3/30	6/60	12/120
GAT+BM3D [13]	No	26.50/0.7249	27.07/0.7587	27.87/0.7849	28.43/0.7962
DN-ResNet-13+‘edge-a’	Yes	<b>27.15/0.7677</b>	<b>27.59/0.7844</b>	<b>28.50/0.8068</b>	<b>28.77/0.8180</b>
DS-DN-ResNet-13+‘edge-a’	Yes	27.11/0.7666	27.53/0.7839	28.45/0.8061	28.68/0.8177

**Table 5.** PSNR (dB)/SSIM evaluation of different blind Gaussian/Poisson denoising methods on multiple datasets. The speed is tested in single Titan-X GPU and  $512 \times 512$  image.

Gaussian sigma=50	Set14	BSD200	VOC2010	Network Size	Speed(ms)
MemNet [22]	26.99/0.7794	25.89/0.7207	27.02/0.7422	667K	343.28
DN-CNN [26]	27.05/0.7788	25.83/0.7214	26.85/0.7439	650K	55.44
DN-ResNet-13+‘edge-a’	<b>27.15/0.7849</b>	<b>25.99/0.7270</b>	<b>27.41/0.7499</b>	149K	17.92
DS-DN-ResNet-13+‘edge-a’	27.05/0.7826	25.87/0.7247	27.32/0.7484	<b>64K</b>	<b>8.33</b>
Poisson peak=8	Set14	BSD200	VOC2010	Network Size	Speed(ms)
MemNet [22]	25.14/0.7198	25.77/0.7031	26.34/0.7321	667K	343.28
DN-ResNet-13+‘edge-a’	<b>25.25/0.7242</b>	<b>25.91/0.7075</b>	<b>26.71/0.7388</b>	149K	55.44
DS-DN-ResNet-13+‘edge-a’	25.10/0.7220	25.79/0.7061	26.60/0.7374	<b>64K</b>	<b>8.33</b>

ing algorithms. Compared to the 20-layer DN-CNN-S [26], DenoiseNet [15], and MemNet [22] which contain more than 600K parameters, DN-ResNet achieves competitive performance, but the network size (150K parameters) is x4 times smaller. DN-ResNet takes 15-20ms to process a  $512 \times 512$  image on single Titan X GPU, compared to 50-60ms for DN-CNN and DenoiseNet. DS-DN-ResNet only takes 8-10ms to process a  $512 \times 512$  image, with the cost of less than 0.1 dB accuracy loss. These results show the effectiveness of DN-ResNet for Gaussian denoising. Example outputs are given in Fig. 7.

In Table 5, we also give the Gaussian and Poisson denoising results on other datasets, Set14, and BSD. The observation is consistent to PASCAL VOC datasets, where DN-ResNet and DS-DN-ResNet still achieve better accuracy. As summary, the proposed DN-ResNet and DS-DN-ResNet achieve the state of art performance for Gaussian/Poisson/Poisson-Gaussian denoising, with better efficiency and smaller network size compared to existing deep CNNs. They are effective for both blind denoising and non-blind denoising.

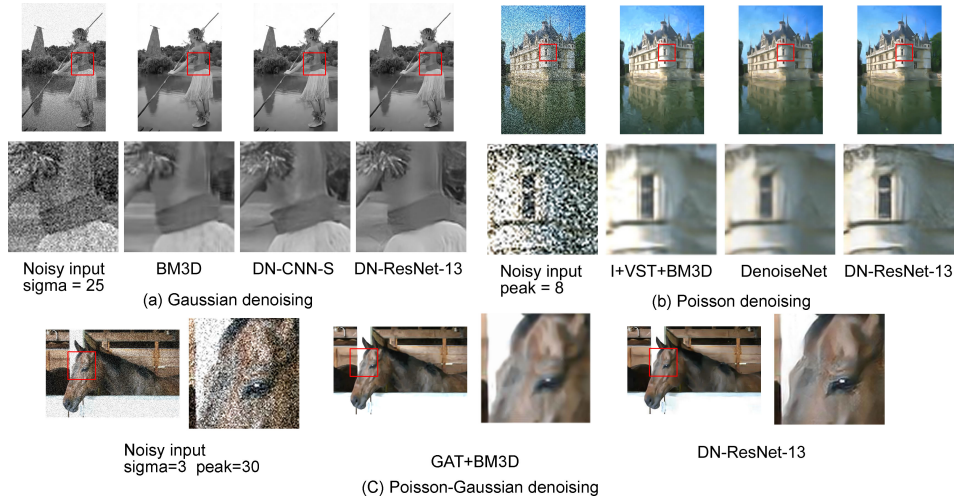


**Fig. 7.** Example outputs of different algorithms for Gaussian, Poisson, and Poisson-Gaussian denoising.

#### 4.4 Experiments on compressed image restoration

Besides image denoising, we also evaluate the proposed DN-ResNet on compressed image restoration. In Fig. 8, the curves of compression ratio (bpp, bit per pixel) versus PSNR of the decoded compressed image and restored image are given. We can find that DN-ResNet is able to improve the quality of the decoded images for all compression methods. 1-2 dB, 0.5-0.7 dB, and 0.3-0.4 dB gain can be observed for JPEG, JPEG 2000, and BPG respectively. Fig. 9 shows some restored images at 0.15 bit per pixel, where DN-ResNet clearly improves the perceptive quality of the decoded compressed images.

Actually, our network can also be applied for image super resolution. We cascade our DN-ResNet to 19 layers and apply it for image super resolution [17]. The low-resolution images are considered as noisy input, and the high-resolution images are considered as clean image. We observe that our DN-ResNet also achieves better PSNR and SSIM for all the scale 2,3,4 in Set 5 and Set 14, but the network size is still 1/3 compared to existing networks such as MemNet [22] or DRRN [21]. This indicates that our DN-ResNet can be utilized as a unified framework for image enhancement.

## 5 Conclusion

In this paper, we presented the DN-ResNet for image denoising achieving both high accuracy and efficiency. We show that cascade training is effective in training efficient deep ResNets. The perceptive quality can be enhanced by using edge-aware loss function. We further propose the depthwise separable ResBlock

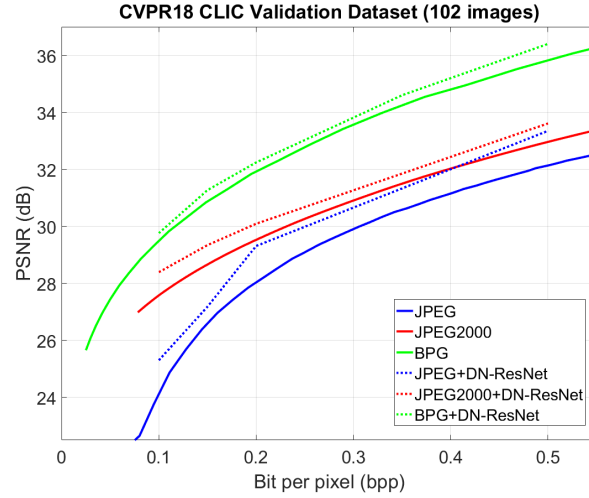


**Fig. 8.** Bit per pixel vs. PSNR in CLIC validation dataset.

and incrementally evolve the DN-ResNet to DS-DN-ResNet. The computational cost of DN-ResNet is reduced 2.5 times, with less than 0.1 dB PSNR loss. Experimental results on benchmark datasets show that for either blind or non-blind denoising, the proposed DN-ResNet achieves better accuracy and efficiency compared to the state of art denoising networks on all types of noises, including Gaussian, Poisson, and Poisson-Gaussian. The same network architecture can be utilized for other image enhancement applications as well.

## References

1. Azzari, L., Foi, A.: Variance stabilization for noisy+ estimate combination in iterative Poisson denoising. *IEEE signal processing letters* **23**(8), 1086–1090 (2016)
2. Burger, H.C., Schuler, C.J., Harmeling, S.: Image denoising: Can plain neural networks compete with BM3D? In: *IEEE Conference on Computer Vision and Pattern Recognition* (2012)
3. Chen, Y., Pock, T.: Trainable nonlinear reaction diffusion: A flexible framework for fast and effective image restoration. *IEEE Transactions on pattern analysis and machine intelligence* **39**(6), 1256–1272 (2017)
4. Dabov, K., Foi, A., Katkovnik, V., Egiazarian, K.: Image denoising by sparse 3-D transform-domain collaborative filtering. *IEEE Transactions on image processing* **16**(8), 2080–2095 (2007)
5. Dong, W., Zhang, L., Shi, G., Li, X.: Nonlocally centralized sparse representation for image restoration. *IEEE Transactions on Image Processing* **22**(4), 1620–1630 (2013)
6. Everingham, M., Van Gool, L., Williams, C.K., Winn, J., Zisserman, A.: The pascal visual object classes (VOC) challenge. *International journal of computer vision* **88**(2), 303–338 (2010)

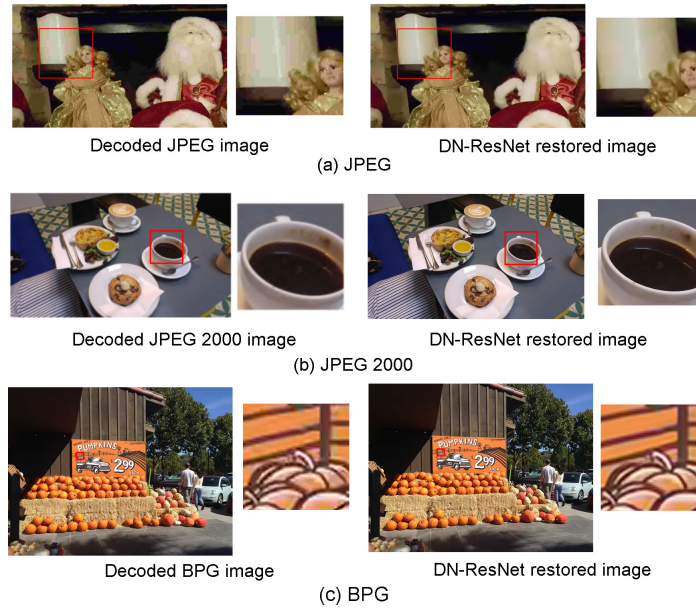


**Fig. 9.** Example outputs of DN-ResNet for compressed image restoration at 0.15 bpp.

7. Foi, A., Trimeche, M., Katkovnik, V., Egiazarian, K.: Practical poissonian-gaussian noise modeling and fitting for single-image raw-data. *IEEE Transactions on Image Processing* **17**(10), 1737–1754 (2008)
8. Gu, S., Zhang, L., Zuo, W., Feng, X.: Weighted nuclear norm minimization with application to image denoising. In: *IEEE Conference on Computer Vision and Pattern Recognition* (2014)
9. He, K., Zhang, X., Ren, S., Sun, J.: Deep residual learning for image recognition. In: *IEEE conference on computer vision and pattern recognition* (2016)
10. Howard, A.G., Zhu, M., Chen, B., Kalenichenko, D., Wang, W., Weyand, T., Andreetto, M., Adam, H.: Mobilenets: Efficient convolutional neural networks for mobile vision applications. *arXiv:1704.04861* (2017)
11. <http://www.compression.cc/>: Workshop and challenge on learned image compression (clic) (2018)
12. Lim, B., Son, S., Kim, H., Nah, S., Lee, K.M.: Enhanced deep residual networks for single image super-resolution. In: *IEEE Conference on Computer Vision and Pattern Recognition Workshops* (2017)
13. Makitalo, M., Foi, A.: Optimal inversion of the generalized Anscombe transformation for Poisson-Gaussian noise. *IEEE Transactions on image processing* **22**(1), 91–103 (2013)
14. Martin, D., Fowlkes, C., Tal, D., Malik, J.: A database of human segmented natural images and its application to evaluating segmentation algorithms and measuring ecological statistics. In: *IEEE International Conference on Computer Vision*. vol. 2, pp. 416–423 (2001)
15. Remez, T., Litany, O., Giryes, R., Bronstein, A.M.: Deep class-aware image denoising. In: *International Conference on Sampling Theory and Applications* (2017)

16. Remez, T., Litany, O., Giryas, R., Bronstein, A.M.: Deep convolutional denoising of low-light images. *arXiv:1701.01687* (2017)
17. Ren, H., El-Khamy, M., Lee, J.: Image super resolution based on fusing multiple convolution neural networks. In: 2017 IEEE Conference on Computer Vision and Pattern Recognition Workshops (CVPRW). pp. 1050–1057. IEEE (2017)
18. Ren, H., El-Khamy, M., Lee, J.: CT-SRCNN: Cascade trained and trimmed deep convolutional neural networks for image super resolution (2018)
19. Sandler, M., Howard, A., Zhu, M., Zhmoginov, A., Chen, L.C.: Mobilenetv2: Inverted residuals and linear bottlenecks. In: IEEE conference on computer vision and pattern recognition (2018)
20. Schmidt, U., Jancsary, J., Nowozin, S., Roth, S., Rother, C.: Cascades of regression tree fields for image restoration. *IEEE Transactions on pattern analysis and machine intelligence* **38**(4), 677–689 (2016)
21. Tai, Y., Yang, J., Liu, X.: Image super-resolution via deep recursive residual network (2017)
22. Tai, Y., Yang, J., Liu, X., Xu, C.: Memnet: A persistent memory network for image restoration. In: Proceedings of the IEEE Conference on Computer Vision and Pattern Recognition. pp. 4539–4547 (2017)
23. Theis, L., Shi, W., Cunningham, A., Huszár, F.: Lossy image compression with compressive autoencoders. *arXiv:1703.00395* (2017)
24. Toderici, G., Vincent, D., Johnston, N., Hwang, S.J., Minnen, D., Shor, J., Covell, M.: Full resolution image compression with recurrent neural networks. In: IEEE conference on computer vision and pattern recognition. pp. 5435–5443 (2017)
25. Zeyde, R., Elad, M., Protter, M.: On single image scale-up using sparse-representations pp. 711–730 (2010)
26. Zhang, K., Zuo, W., Chen, Y., Meng, D., Zhang, L.: Beyond a gaussian denoiser: Residual learning of deep cnn for image denoising. *IEEE Transactions on Image Processing* **26**(7), 3142–3155 (2017)
27. Zhang, K., Zuo, W., Zhang, L.: FFDnet: Toward a fast and flexible solution for cnn based image denoising. *arXiv:1710.04026* (2017)